

was depleted) cell death was reduced (67 to 16%) (Fig. 4C). Similar schedule-dependent interactions were observed between MDMX suppression and four different chemotherapy agents (4NQO, doxorubicin, camptothecin, and actinomycin D) in MCF7 and the primary line RPE1 (fig. S7).

MDMX-depleted cells showed a similar amplitude of p53 accumulation to that in mock-treated cells when DNA damage was applied during phase II (Fig. 4, E, H, and I, and fig. S6B), indicating that the reduction in cell death is not caused by lower amounts of p53. Instead, we suggest that transcriptional regulation of genes by MDMX-induced p53 oscillations could make cells less susceptible to DNA damage. Indeed, p53 oscillations during the second phase after MDMX depletion induced accumulation of p21 and cell cycle arrest (Fig. 3, D and E), which provides protection from cell death (17). In addition, MDMX suppression led to a stronger activation of the pro-survival signal phospho-Akt after DNA damage and to a weaker accumulation of the pro-apoptotic protein PUMA as compared with those in MDMX-expressing cells (fig. S8). This suggests that, in addition to induction of p21 and cell cycle arrest by p53 oscillations, MDMX suppression shifts cells toward a pro-survival cellular state (fig. S8), which may also contribute to its protection from DNA damage-induced cell death.

The complexity of cellular signaling pathways makes it challenging to predict the response to a single perturbation, and even more challenging to predict responses to combined perturbations. In the context of combined therapeutic treatments, the schedule of administration can be crucial [Fig. 4J and (1, 18, 19)]. The results presented here unexpectedly show that the combination of DNA damage with MDMX inhibitors for cancer therapy has the potential either to improve cancer therapy or to blunt its effects. Our results have implications for the design of MDMX-combination drug regimes and perhaps for the design of combination therapies in general. Further consideration of treatment schemes in the context of other physiological rhythms, such as the cell cycle and circadian clock (20–22), can be critical for more precise and effective therapies. Such a detailed quantitative description of system behavior at the single-cell level can reveal hidden regulatory principles and the nature of cellular state changes in response to perturbations.

REFERENCES AND NOTES

- M. J. Lee *et al.*, *Cell* **149**, 780–794 (2012).
- S. W. Morton *et al.*, *Sci. Signal.* **7**, ra44 (2014).
- M. Wade, Y.-C. Li, G. M. Wahl, *Nat. Rev. Cancer* **13**, 83–96 (2013).
- A. Gembarska *et al.*, *Nat. Med.* **18**, 1239–1247 (2012).
- C. J. Brown, S. Lain, C. S. Verma, A. R. Fersht, D. P. Lane, *Nat. Rev. Cancer* **9**, 862–873 (2009).
- J. A. Barboza, T. Iwakuma, T. Terzian, A. K. El-Naggar, G. Lozano, *Mol. Cancer Res.* **6**, 947–954 (2008).
- F. Mancini *et al.*, *Int. J. Biochem. Cell Biol.* **42**, 1080–1083 (2010).
- X. Wang, J. Wang, X. Jiang, *J. Biol. Chem.* **286**, 23725–23734 (2011).
- J. E. Purvis *et al.*, *Science* **336**, 1440–1444 (2012).
- B. Graves *et al.*, *Proc. Natl. Acad. Sci. U.S.A.* **109**, 11788–11793 (2012).
- D. Reed *et al.*, *J. Biol. Chem.* **285**, 10786–10796 (2010).
- G. Lahav *et al.*, *Nat. Genet.* **36**, 147–150 (2004).
- A. Loewer, E. Batchelor, G. Gaglia, G. Lahav, *Cell* **142**, 89–100 (2010).
- E. Batchelor, C. S. Mock, I. Bhan, A. Loewer, G. Lahav, *Mol. Cell* **30**, 277–289 (2008).
- H. Kawai *et al.*, *J. Biol. Chem.* **278**, 45946–45953 (2003).
- G. Lahav, *Adv. Exp. Med. Biol.* **641**, 28–38 (2008).
- O. D. K. Maddocks *et al.*, *Nature* **493**, 542–546 (2013).
- M. Behar, D. Barken, S. L. Werner, A. Hoffmann, *Cell* **155**, 448–461 (2013).
- P. Lito, N. Rosen, D. B. Solit, *Nat. Med.* **19**, 1401–1409 (2013).
- J. Bieler *et al.*, *Mol. Syst. Biol.* **10**, 739 (2014).
- C. Feillet *et al.*, *Proc. Natl. Acad. Sci. U.S.A.* **111**, 9828–9833 (2014).
- A. Sancar *et al.*, *FEBS Lett.* **584**, 2618–2625 (2010).

ACKNOWLEDGMENTS

We thank A. G. Jochemsen, J. C. Marine, X. Wang, and J. Chen for sharing their experience and thoughts on MDMX regulation; R. Ward, S. Gruver, G. Gaglia, J. Porter, L. Bruett, and members of the Lahav laboratory for comments, support, and discussion; and the Nikon Imaging Center at Harvard Medical School for support with live cell imaging. This research was supported by National Institutes of Health grant GM083303 to G.L., grant F32GM105205 to S.C., and funding from the Novartis Institutes for Biomedical Research.

SUPPLEMENTARY MATERIALS

www.sciencemag.org/content/351/6278/1204/suppl/DC1
Materials and Methods
Figs. S1 to S8
References (23–25)

12 May 2015; accepted 28 January 2016
10.1126/science.aac5610

CANCER THERAPY

Disordered methionine metabolism in MTAP/CDKN2A-deleted cancers leads to dependence on PRMT5

Konstantinos J. Mavrakis,^{1*} E. Robert McDonald III,^{1*} Michael R. Schlabach,^{1*} Eric Billy,^{2*} Gregory R. Hoffman,^{1*} Antoine deWeck,² David A. Ruddy,¹ Kavitha Venkatesan,¹ Jianjun Yu,³ Gregg McAllister,¹ Mark Stump,¹ Rosalie deBeaumont,¹ Samuel Ho,¹ Yingzi Yue,¹ Yue Liu,¹ Yan Yan-Neale,¹ Guizhi Yang,¹ Fallon Lin,¹ Hong Yin,¹ Hui Gao,¹ D. Randal Kipp,¹ Songping Zhao,¹ Joshua T. McNamara,¹ Elizabeth R. Sprague,¹ Bing Zheng,³ Ying Lin,⁴ Young Shin Cho,¹ Justin Gu,⁴ Kenneth Crawford,³ David Ciccone,¹ Alberto C. Vitari,³ Albert Lai,³ Vladimir Capka,¹ Kristen Hurov,¹ Jeffery A. Porter,¹ John Tallarico,¹ Craig Mickanin,¹ Emma Lees,¹ Raymond Pagliarini,¹ Nicholas Keen,¹ Tobias Schmelzle,^{2*} Francesco Hofmann,^{2*} Frank Stegmeier,^{1*†} William R. Sellers^{1*†}

5-Methylthioadenosine phosphorylase (MTAP) is a key enzyme in the methionine salvage pathway. The *MTAP* gene is frequently deleted in human cancers because of its chromosomal proximity to the tumor suppressor gene *CDKN2A*. By interrogating data from a large-scale short hairpin RNA-mediated screen across 390 cancer cell line models, we found that the viability of MTAP-deficient cancer cells is impaired by depletion of the protein arginine methyltransferase PRMT5. MTAP-deleted cells accumulate the metabolite methylthioadenosine (MTA), which we found to inhibit PRMT5 methyltransferase activity. Deletion of MTAP in MTAP-proficient cells rendered them sensitive to PRMT5 depletion. Conversely, reconstitution of MTAP in an MTAP-deficient cell line rescued PRMT5 dependence. Thus, MTA accumulation in MTAP-deleted cancers creates a hypomorphic PRMT5 state that is selectively sensitized toward further PRMT5 inhibition. Inhibitors of PRMT5 that leverage this dysregulated metabolic state merit further investigation as a potential therapy for MTAP/CDKN2A-deleted tumors.

5-Methylthioadenosine phosphorylase (MTAP) participates in the methionine salvage pathway that metabolizes methylthioadenosine (MTA) to adenine and methionine. Because of its proximity to the tumor suppressor gene *CDKN2A* on human chromosome 9p21, the *MTAP* gene is deleted at high frequency in many human tumors, including 53% of glioblastomas, 26% of pancreatic cancers, and other tumor types (Fig. 1A). Given the critical role of MTAP in methionine metabolism, we hypothesized that the

metabolic rewiring in response to MTAP loss may create new vulnerabilities.

¹Novartis Institutes for Biomedical Research, Cambridge, MA 02139, USA. ²Novartis Institutes for Biomedical Research, Basel CH-4002, Switzerland. ³Novartis Institutes for Biomedical Research, Emeryville, CA 94608, USA. ⁴China Novartis Institutes for Biomedical Research, Shanghai 201203, China.

*These authors contributed equally to this work. †Corresponding authors. E-mail: william.sellers@novartis.com (W.R.S.); fstegmeier@ksqtx.com (F.S.)

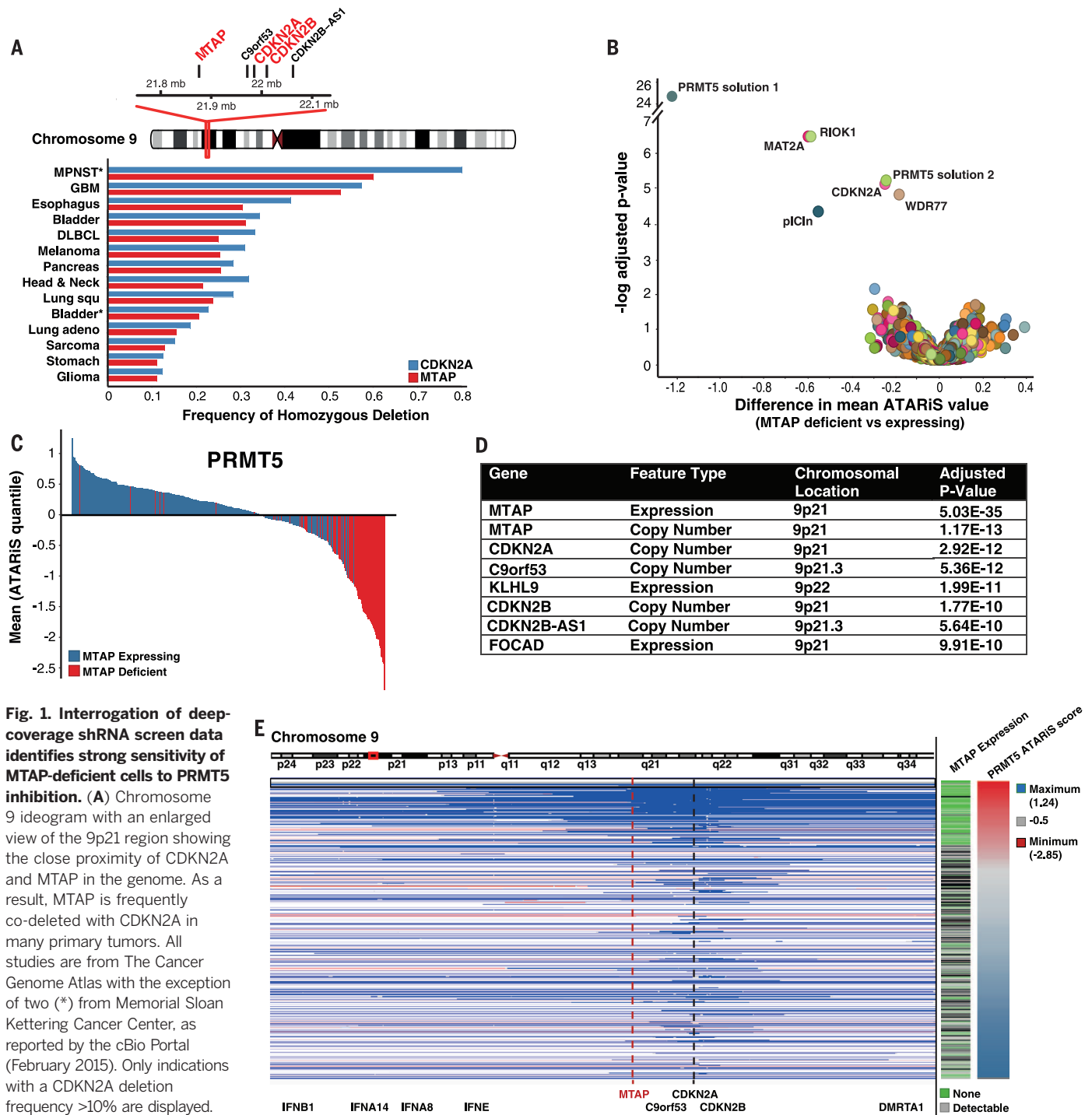


Fig. 1. Interrogation of deep-coverage shRNA screen data identifies strong sensitivity of MTAP-deficient cells to PRMT5 inhibition. (A) Chromosome 9 ideogram with an enlarged view of the 9p21 region showing the close proximity of CDKN2A and MTAP in the genome. As a result, MTAP is frequently co-deleted with CDKN2A in many primary tumors. All studies are from The Cancer Genome Atlas with the exception of two (*) from Memorial Sloan Kettering Cancer Center, as reported by the cBio Portal (February 2015). Only indications with a CDKN2A deletion frequency >10% are displayed.

(B) Pooled shRNA screen analysis to identify genes that are selectively required for the proliferation of cells lacking MTAP expression. The mean difference in gene-level ATARIS scores between MTAP-deficient and MTAP-expressing cells is plotted on the x axis, and the degree of significance is on the y axis (P values calculated by Mann-Whitney-Wilcoxon rank sum test and adjusted by the false-discovery rate). Note that two independent gene-level solutions for PRMT5 (PRMT5 solution 1 and PRMT5 solution 2, as computed by ATARIS algorithm) scored as differentially lethal in MTAP-deficient versus MTAP-expressing setting. (C) Waterfall plot of PRMT5 dependence colored by MTAP RNA expression [MTAP deficient (<4.5) in red and MTAP expressing (>4.5) in blue]. (D) Unbiased correlation analysis of predictors of PRMT5

dependence across all CCLE features, including mutations, copy number, and expression—the most significantly associated features are listed; P values have been corrected for multiple-hypothesis testing, and, e.g., $P = 5.03E-35$ may be stated $P = 5.03 \times 10^{-35}$. (E) The Integrative Genomics Viewer chromosomal view of the 9p21.3 locus across the panel of screened cell lines, sorted according to their sensitivity to PRMT5 depletion. Cell line models that are most dependent on PRMT5 are at the top (minimum ATARIS score) and least-dependent cell lines at the bottom (maximum ATARIS score). MTAP expression (RNA) is co-plotted as a heat map. Broader deletions encompassing both MTAP and CDKN2A lead to a loss of MTAP expression (green) and PRMT5 sensitivity (red).

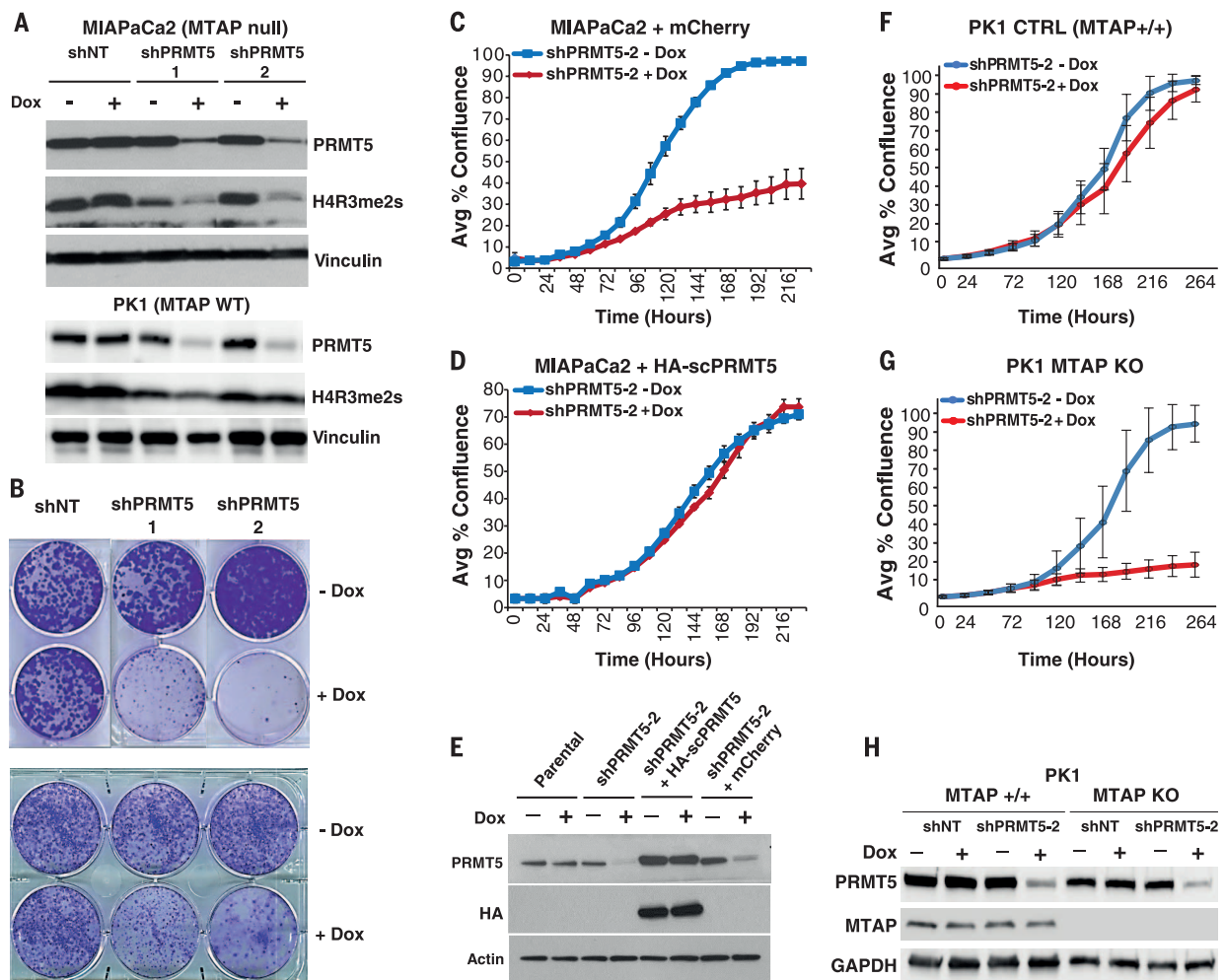


Fig. 2. Loss of MTAP renders cells sensitive to PRMT5 depletion. (A) Immunoblot to assess PRMT5 depletion of two independent doxycycline (Dox)–inducible hairpins (shPRMT5-1 and shPRMT5-2); shNT represents a nontargeting control shRNA. PRMT5 protein levels and H4R3me2s were assessed by immunoblotting in MTAP-null (MIAPaCa2) and MTAP-expressing (WT; PK1) pancreatic cell lines. Vinculin serves as a loading control. (B) Foci-formation assays of cell lines [corresponding to Western blots in (A)] transduced with the indicated inducible shRNAs. (C) shRNA-mediated depletion of PRMT5 substantially decreased the confluence (measured by IncuCyte) of MIAPaCa2 shPRMT5-2 cells stably expressing an empty control vector (mCherry); –Dox (blue) versus +Dox (red); $P < 0.001$. (D) Expression of a shRNA-resistant PRMT5 cDNA (HA-scPRMT5) fully rescued the antiproliferative effects of PRMT5 shRNA (NS, $P > 0.05$;

shown are means and SD of triplicate experiments). (E) Immunoblot of lysates extracted from MIAPaCa2 (parental), MIAPaCa2 stably expressing shPRMT5-2, and stable MIAPaCa2 shPRMT5-2 cell lines expressing either HA-scPRMT5 or mCherry control that were probed for PRMT5, HA, and actin loading control. (F and G) In vitro proliferation assay of PK1 MTAP isogenic cell lines that have been engineered with a nontargeting control single guide RNA (sgRNA) (PK1 CTRL) (F) or with a sgRNA-targeting MTAP (PK1 MTAP KO) (G) and stably express a Dox-inducible PRMT5 shRNA (shPRMT5-2). The proliferation of cells with and without treatment with doxycycline (\pm Dox) over time (hours) was assessed by IncuCyte ($n = 24$ per treatment condition). (H) Immunoblot of cells used in (F) and (G) with and without shRNA induction and probed with the indicated antibodies.

We recently performed a pooled short hairpin RNA (shRNA) screen across 390 cancer cell lines of the Cancer Cell Line Encyclopedia (CCLE) with a library encompassing ~7500 genes at an approximate depth of 20 shRNAs per gene. To find genes that are selectively required for the viability of MTAP-deficient cells, we compared the gene-level shRNA values [using ATARIS, (1)] between cell line models lacking MTAP expression to those that express MTAP (fig. S1A, table S1, and table S2). This analysis identified several genes that selectively affected the growth of MTAP-deficient cells (Fig. 1B and fig. S2). One

of the hits that scored as selectively lethal to MTAP-deficient cells was methionine adenosyltransferase 2A (MAT2A) ($P = 2.93 \times 10^{-7}$) (Fig. 1B), an enzyme within the *S*-adenosyl methionine (SAM) biosynthesis pathway (fig. S1C), which supported the notion that MTAP loss creates new metabolic vulnerabilities. The most differential hit was the protein arginine methyltransferase PRMT5 ($P = 1.64 \times 10^{-25}$). Several cofactors that are required for PRMT5 function, such as methylosome protein 50 (MEP50/WDR77) ($P = 1.21 \times 10^{-5}$), methylosome subunit pICln ($P = 3.81 \times 10^{-5}$), and RIO kinase 1 (RIOK1) ($P =$

2.93×10^{-7}) (2, 3), also scored as differentially required for the growth of MTAP-deficient cancer cells (Fig. 1B). Similar results were obtained when the cell lines were partitioned by MTAP copy number rather than by expression values (fig. S1B).

To test the hypothesis that the PRMT5 complex is selectively required for the proliferation of MTAP-deficient cells, we performed a reciprocal unbiased correlation analysis of all CCLE features (including somatic mutations, copy number, and expression data) to identify which markers correlate best with PRMT5 dependence.

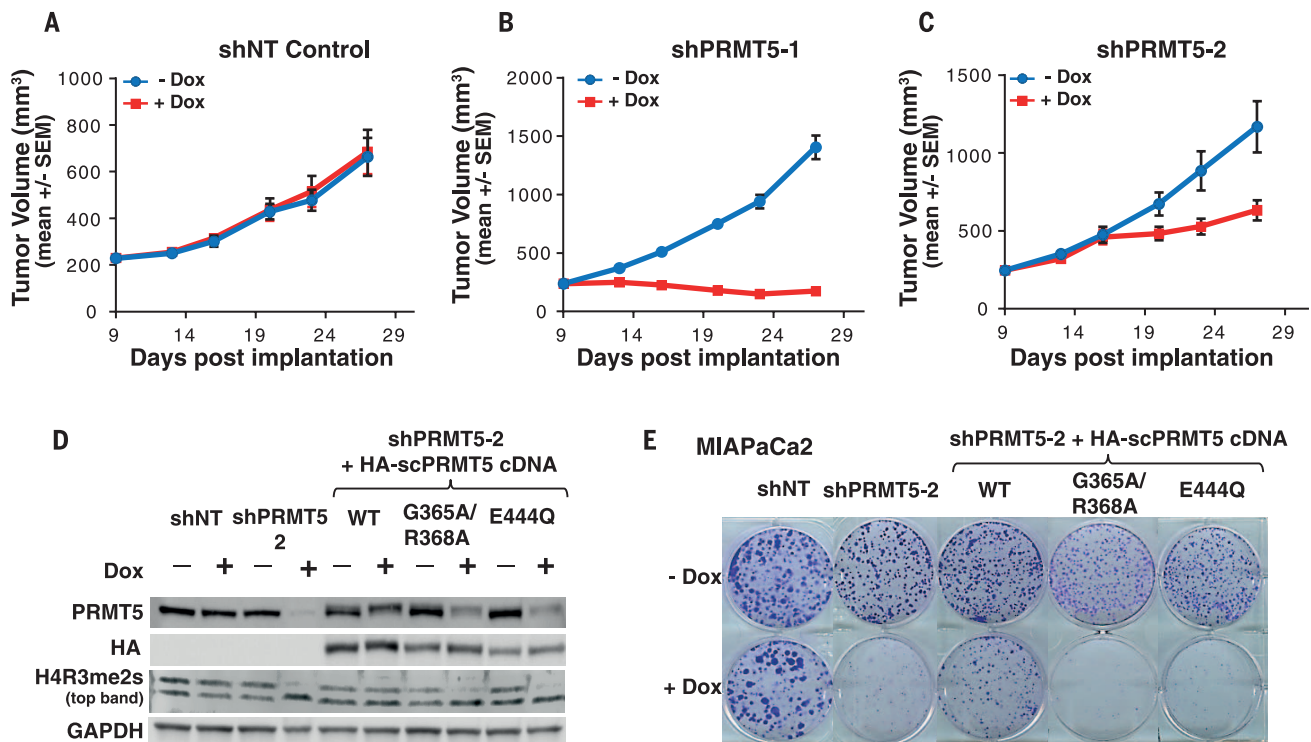


Fig. 3 PRMT5 is required for the growth of MTAP-deficient cells in vivo, and its catalytic HMT activity is essential. (A to C) MIAPaCa2 cells stably expressing shNT (A) or one of two inducible PRMT5 shRNAs—(B) shPRMT5-1 and (C) shPRMT5-2—were subcutaneously implanted, and tumor volume was monitored over a 28-day period. Dox treatment was initiated on day 9 postimplantation (± 7 for each treatment arm; shown are mean tumor volumes and SEM). shNT control +Dox (red) versus -Dox (blue) ($P = 0.943$); shPRMT5-1 \pm Dox ($P < 0.001$); shPRMT5-2 \pm Dox ($P < 0.001$). (D and E) PRMT5

catalytic activity is required for growth in MTAP-deficient MIAPaCa2 cells. (D) Immunoblot of stable lines generated with shRNA-resistant mutants and probed with antibodies detecting PRMT5, HA, H4R3me2s, and glyceraldehyde-3-phosphate dehydrogenase (GAPDH) loading control. (E) Cells were transfected with the indicated shRNAs and shRNA-resistant cDNA vectors, and the relative growth was assessed by foci-formation assay. WT denotes wild-type PRMT5. G365A/R368A and E444Q are catalytically inactive PRMT5 mutants.

This analysis revealed deletion (low copy number) of *MTAP* ($P = 1.17 \times 10^{-13}$) and low expression ($P = 5.03 \times 10^{-35}$) of *MTAP* as the top features predictive of cancer cell dependence on PRMT5 (Fig. 1, C and D, and fig. S1D), followed by deletion of *CDKN2A* and *CDKN2B*. Although cells with concomitant loss of both *CDKN2A* and *MTAP* were strongly sensitive to PRMT5 depletion (knockdown), cells harboring focal deletions encompassing *CDKN2A*, but not *MTAP*, were generally insensitive to PRMT5 depletion (Fig. 1E). These findings indicate that loss of *MTAP*, rather than *CDKN2A*, confers sensitivity to PRMT5 inhibition. Thus, PRMT5 dependence is an example of collateral lethality (4) in which *MTAP* loss, as a consequence of *CDKN2A* deletion, creates a selective vulnerability to PRMT5 knockdown.

We next explored the mechanistic link between *MTAP* loss and PRMT5 knockdown. Knockdown of PRMT5 with two independent shRNAs (fig. S3, A and B, and fig. S4, A and B) markedly inhibited cell growth in two pancreatic *MTAP*-null cell line models, MIAPaCa2 and su86.86 (Fig. 2B and fig. S5). By contrast, PRMT5 depletion had only minor effects on viability in the *MTAP*-expressing pancreatic cell line PK1, de-

spite displaying similar levels of PRMT5 protein knockdown (Fig. 2, A and B, and fig. S5, A to C). Expression of a shRNA-resistant version of PRMT5 fully rescued the colony formation and proliferation effects in MIAPaCa2, which indicated that growth inhibition is mediated by PRMT5 depletion and is unlikely to be a consequence of shRNA off-target effects (Fig. 2, C to E). To directly test the hypothesis that *MTAP* loss confers sensitivity to PRMT5 knockdown, we next evaluated the effect of PRMT5 depletion in an isogenic cell line setting. To this end, clustered regularly interspaced short palindromic repeats (CRISPR)-mediated deletion was used to inactivate *MTAP* in PK1 cells. In comparison with parental PK1 cells, PK1-*MTAP*^{-/-} cells were strongly sensitized to shRNAs targeting PRMT5 (Fig. 2, F to H, and fig. S6, A to D). To examine if *MTAP*-deficient cells remained dependent on PRMT5 in vivo, we established tumor xenografts of the *MTAP*-deficient MIAPaCa2 cells expressing inducible shRNAs targeting PRMT5 or a nontargeting control and monitored tumor size over time. Induction of PRMT5 shRNAs led to reduced levels of H4R3me2s (symmetrical dimethylation on arginine 3 of histone 4), a known PRMT5 substrate (5–7), and markedly inhibited

tumor growth, whereas the nontargeting control had no impact on tumor volume (Fig. 3, A to C, and fig. S7E). In keeping with the in vitro observations, this effect was specific to cells with *MTAP* loss, as PRMT5 knockdown did not affect the growth of the *MTAP*-expressing HARA xenograft model (fig. S7, A to D). Similar in vivo results were obtained with the PK1 *MTAP* isogenic cell lines, which confirmed that loss of *MTAP* is responsible for the difference in sensitivity (fig. S8). These experiments indicate that *MTAP*-deficient cells are sensitive to PRMT5 inhibition in vitro and in vivo.

We examined whether the methyltransferase activity of PRMT5 was required for the growth of *MTAP*-deficient cells. Expression of PRMT5 mutant proteins predicted to affect SAM binding (G365A/R368A; in which alanine replaces glycine 365 and arginine 368) or the methyltransferase activity (E444Q; in which glutamine replaced Glu⁴⁴⁴) (3, 8, 9) failed to restore H4R3me2s levels in cells depleted for endogenous PRMT5, which confirmed their impaired catalytic activity (Fig. 3D). Despite being expressed at levels similar to those of wild-type PRMT5, the two catalytically dead PRMT5 mutants failed to rescue the growth of PRMT5-depleted cells (Fig. 3E), which

indicated that the catalytic activity of PRMT5 is required for the proliferation of MTAP-deficient cells. It remained unclear, however, why cancer cells lacking MTAP are selectively sensitized toward PRMT5 depletion mediated by RNA interference (RNAi). MTAP catalyzes the phosphorylation of MTA to adenine and 5-methylthioribose-1-phosphate, which is further recycled to methionine (10) (fig. S1C), and tumors with loss of MTAP exhibit a marked increase of intra- and extracellular levels of MTA (5, 11, 12). Consistent with the prior tumor data, metabolic profiling of MTA across a number of MTAP-deficient and -proficient cancer models, as well as in the PK1 isogenic cell lines, revealed that both intra- and extracellular MTA levels were increased in cells lacking MTAP (Fig. 4A; fig. S9, A and B; and fig. S10B). By contrast, intracellular SAM levels were on average higher than MTA levels and did not stratify with MTAP status (fig. S10, A and B). Given that MTA has been proposed to act as a general inhibitor of PRMTs (12, 13), we hypothesized that increased MTA levels due to MTAP loss may partially cripple PRMT5 catalytic activity and thereby sensitize cells to further PRMT5 inhibition. Indeed, deletion of MTAP in PK1 cells (MTAP-KO) led to a reduction in the levels of H4R3me2s, consistent with the hypothesis that MTAP loss leads to reduced PRMT5 activity (Fig. 4B). Conversely, reexpression of MTAP in the MTAP-deficient MIA PaCa2 cell line, which according to our model should restore PRMT5 function by lowering MTA levels, resulted in increased levels of H4R3me2s (Fig. 4C).

To investigate the inhibitory activity of MTA on PRMTs in more detail, we profiled MTA in biochemical assays across a panel of 18 histone methyltransferases (HMTs), including several PRMTs (6). In contrast to the pan-methyltransferase inhibitor sinefungin (7), MTA selectively inhibited PRMT5 activity with a median inhibitory concentration (IC_{50}) of 4.6 μ M and did not affect the activity of any of the other methyltransferases profiled at concentrations up to 100 μ M (Fig. 4D and table S3). This finding may help explain why MTAP-deficient cells are selectively sensitized to depletion of PRMT5 but not other PRMT family members.

To further investigate the selective inhibition of PRMT5 by MTA, we determined the crystal structure of MTA-bound PRMT5:WDR77 in complex with a H4 peptide (Fig. 4E and table S7). SAM and MTA are structurally similar (fig. S10C), and as expected, the adenine and ribose moieties of MTA are nearly identical to those described for the SAM analog (A9145C) bound to human PRMT5:WDR77 (3). Our analysis revealed a change in the conformation of Glu⁴³⁵ in the MTA-bound form of PRMT5; this residue no longer coordinates the arginine residue of the peptide substrate as seen in the A9145C-peptide structure (Fig. 4E; cyan) but, rather, shifts down to make a split hydrogen bond with Tyr³³⁴ and a salt bridge with Lys³³³ (Fig. 4E; purple). The shifted Glu⁴³⁵ side chain and an additional water molecule occupy a region similar to the 2-aminobutanoate

of the SAM analog, and they form the lower wall of the MTA pocket. Whereas Glu⁴³⁵ is invariant among all arginine methyltransferase family members and has been proposed to be important for function, Lys³³³ and Tyr³³⁴ are unique to PRMT5 (Fig. 4E). Thus, we hypothesize that the selectivity of MTA inhibition for PRMT5 is due, in part, to the reordering of the cofactor binding pocket facilitated by the Glu⁴³⁵-Lys³³³/Tyr³³⁴ interactions.

If MTAP loss, and concomitant MTA accumulation, is responsible for inducing sensitivity to PRMT5 inhibition, then restoration of MTAP function should render MTAP-deficient cells insensitive to PRMT5 depletion. Indeed, expression of exogenous MTAP in the MTAP-deficient MIA PaCa2 cell line rescued the PRMT5 shRNA-mediated effects on proliferation (Fig. 4, F and G). Moreover, MTA supplementation resensitized this MTAP-reconstituted cell line to PRMT5 knockdown, which resulted in decreased proliferation and H4R3me2s levels (Fig. 4, H to J, and fig. S11, A and B). Higher concentrations of MTA (25 μ M MTA) (Fig. 4J) by itself caused antiproliferative effects and reduced H4R3me2s to levels comparable to those seen with PRMT5 knockdown in the MIA PaCa2 wild-type (WT) scenario (fig. S11C). This effect could either be due to more complete inhibition of PRMT5 function, thus mimicking the PRMT5 null phenotype, or might be mediated by feedback inhibition of spermidine synthase, a by-product of polyamine synthesis (10, 14, 15).

EPZ015666 is a potent pharmacological inhibitor of PRMT5, and it requires SAM for efficient binding to and inhibition of the enzyme (16). SAM is more abundant than MTA in cells. Whereas MTAP loss leads to a profound increase in MTA levels (Fig. 4, A and B), we found that it has little impact on SAM levels (fig. S9C and fig. S10, A and B). We hypothesized that the activity of SAM cooperative inhibitors would not be differentially affected by the altered metabolic state in MTAP-deficient cancers. Indeed, when we profiled EPZ015666 across a panel of 11 MTAP-deficient and intact cell lines, including the PK1 isogenic MTAP-KO cells, we did not detect substantial selective antiproliferative effects correlating with MTAP status (fig. S12, A to D). Consistent with this, we found that complete inactivation of PRMT5 by CRISPR is lethal even in MTAP-proficient cells (fig. S13, A to C). PRMT5 biochemical assays with differing concentrations of MTA and SAM (fig. S14A) further supported our hypothesis.

Because MTA inhibits PRMT5 by competing rather than cooperating with SAM for binding to the catalytic site (fig. S14, B and C), we next explored whether MTA itself could act as an exogenous SAM-competitive inhibitor. We found that the isogenic MTAP-deleted PK1 cells were more sensitive to MTA than the parental PK1 cells (Fig. 4K). Therefore, in the MTAP-deleted setting, where an increased fraction of the MTA-bound inactive form of PRMT5 exists, enhanced sensitivity to exogenous MTA is achieved, and this is due to its SAM-competitive binding mode. Thus, we postulate that SAM-competitive inhibition of

PRMT5 can be exploited to selectively alter the proliferation of MTAP-deficient cells. Overall, our data suggest a model in which complete loss of MTAP leads to partial metabolite-based inhibition of PRMT5 by altering the ratio of MTA to SAM (fig. S15).

In summary, loss of the 9p21 tumor suppressor locus is the most common deletion event across all cancer types, yet this event has remained intractable for therapeutic targeting. Our study and that of Kryukov *et al.* (17) indicate that deletion of the *MTAP* gene in human cancer leads to an altered metabolic state that represents an attractive opportunity for therapeutic intervention. Based on our mechanistic insights, therapeutics that mimic the mode of action of MTA on PRMT5 function (e.g., by competing with SAM for binding to PRMT5) or that preferentially bind to PRMT5 in the presence of MTA will be required to pharmacologically exploit the PRMT5 hypomorphic state found in these cancers.

REFERENCES AND NOTES

- D. D. Shao *et al.*, *Genome Res.* **23**, 665–678 (2013).
- G. Guderian *et al.*, *J. Biol. Chem.* **286**, 1976–1986 (2011).
- S. Antonysamy *et al.*, *Proc. Natl. Acad. Sci. U.S.A.* **109**, 17960–17965 (2012).
- F. L. Muller *et al.*, *Nature* **488**, 337–342 (2012).
- A. P. Stevens *et al.*, *J. Cell. Biochem.* **106**, 210–219 (2009).
- W. Qi *et al.*, *Proc. Natl. Acad. Sci. U.S.A.* **109**, 21360–21365 (2012).
- J. Li, J. S. Chorba, S. P. Whelan, *J. Virol.* **81**, 4104–4115 (2007).
- T. L. Branscombe *et al.*, *J. Biol. Chem.* **276**, 32971–32976 (2001).
- M. C. Ho *et al.*, *PLoS ONE* **8**, e57008 (2013).
- L. Christa, L. Thuillier, A. Munier, J. L. Pérignon, *Biochim. Biophys. Acta* **803**, 7–10 (1984).
- I. Basu *et al.*, *J. Biol. Chem.* **282**, 21477–21486 (2007).
- K. Limm *et al.*, *Eur. J. Cancer* **49**, 1305–1313 (2013).
- P. A. Maher, *J. Biol. Chem.* **268**, 4244–4249 (1993).
- L. Christa, J. Kersual, J. Augé, J. L. Pérignon, *Biochem. J.* **255**, 145–152 (1988).
- A. L. Subhi *et al.*, *J. Biol. Chem.* **278**, 49868–49873 (2003).
- E. Chan-Penebre *et al.*, *Nat. Chem. Biol.* **11**, 432–437 (2015).
- G. V. Kryukov *et al.*, *Science* **351**, aad5214 (2016).

ACKNOWLEDGMENTS

Use of the Industrial Macromolecular Crystallography Association Collaborative Access Team (IMCA-CAT) beamline 17-ID (or 17-BM) at the Advanced Photon Source was supported by the companies of the Industrial Macromolecular Crystallography Association through a contract with Hauptman-Woodward Medical Research Institute. Use of the Advanced Photon Source was supported by the Office of Science, Office of Basic Energy Sciences, U.S. Department of Energy, under contract no. DE-AC02-06CH11357. Novartis has filed a patent application relating to the use of inhibitors to treat MTAP-deficient diseases (62/049004).

SUPPLEMENTARY MATERIALS

www.sciencemag.org/351/6278/1208/suppl/DC1
Materials and Methods
Figs. S1 to S15
Tables S1 to S7
Data Tables S8 and S9
References (18–29)

6 October 2015; accepted 1 February 2016
Published online 11 February 2016
10.1126/science.aad5944

Disordered methionine metabolism in MTAP/CDKN2A-deleted cancers leads to dependence on PRMT5

Konstantinos J. Mavrakis, E. Robert McDonald III, Michael R. Schlabach, Eric Billy, Gregory R. Hoffman, Antoine deWeck, David A. Ruddy, Kavitha Venkatesan, Jianjun Yu, Gregg McAllister, Mark Stump, Rosalie deBeaumont, Samuel Ho, Yingzi Yue, Yue Liu, Yan Yan-Neale, Guizhi Yang, Fallon Lin, Hong Yin, Hui Gao, D. Randal Kipp, Songping Zhao, Joshua T. McNamara, Elizabeth R. Sprague, Bing Zheng, Ying Lin, Young Shin Cho, Justin Gu, Kenneth Crawford, David Ciccone, Alberto C. Vitari, Albert Lai, Vladimir Capka, Kristen Hurov, Jeffery A. Porter, John Tallarico, Craig Mickanin, Emma Lees, Raymond Pagliarini, Nicholas Keen, Tobias Schmelzle, Francesco Hofmann, Frank Stegmeier and William R. Sellers

Science **351** (6278), 1208-1213.

DOI: 10.1126/science.aad5944 originally published online February 11, 2016

Tumors put in a vulnerable position

Cancer cells often display alterations in metabolism that help fuel their growth. Such metabolic "rewiring" may also work against the cancer cells, however, by creating new vulnerabilities that can be exploited therapeutically. A variety of human tumors show changes in methionine metabolism caused by loss of the gene coding for 5-methylthioadenosine phosphorylase (MTAP). Mavrakis *et al.* and Kryukov *et al.* found that the loss of MTAP renders cancer cell lines sensitive to growth inhibition by compounds that suppress the activity of a specific arginine methyltransferase called PRMT5. Conceivably, drugs that inhibit PRMT5 activity could be developed into a tailored therapy for MTAP-deficient tumors.

Science, this issue pp. 1208 and 1214

ARTICLE TOOLS

<http://science.sciencemag.org/content/351/6278/1208>

SUPPLEMENTARY MATERIALS

<http://science.sciencemag.org/content/suppl/2016/02/10/science.aad5944.DC1>

RELATED CONTENT

<http://science.sciencemag.org/content/sci/351/6278/1214.full>
<http://stke.sciencemag.org/content/sigtrans/6/268/pe12.full>
<http://stke.sciencemag.org/content/sigtrans/7/319/ra31.full>

REFERENCES

This article cites 29 articles, 13 of which you can access for free
<http://science.sciencemag.org/content/351/6278/1208#BIBL>

PERMISSIONS

<http://www.sciencemag.org/help/reprints-and-permissions>

Use of this article is subject to the [Terms of Service](#)